

Supporting Information

Binding of the Microbial Cyclic Tetrapeptide Trapoxin A to the Class I Histone Deacetylase HDAC8

Nicholas J. Porter and David W. Christianson*

Roy and Diana Vagelos Laboratories, Department of Chemistry, University of Pennsylvania,
Philadelphia, PA 19104-6323, United States

*author to whom correspondence should be sent: E-mail chris@sas.upenn.edu

Materials and Methods

General. Chemicals used in buffers and crystallization were purchased from Fischer, Sigma-Aldrich, or Hampton Research and used without further purification. Each polymerase chain reaction (PCR) was performed using PfuUltra High-Fidelity DNA polymerase (Agilent Technologies). Restriction enzyme SSP1 was purchased from New England Biolabs and used according to the manufacturer's instructions. Oligonucleotides for cloning and mutagenesis were synthesized by Integrated DNA Technologies. All DNA sequences were confirmed at the Genomics Analysis Core, Perelman School of Medicine, University of Pennsylvania. *Escherichia coli* strain DH5 α (Invitrogen) was used for cloning and plasmid preparation. Trapoxin A and apicidin were purchased from Sigma-Aldrich at $\geq 98\%$ purity. Coumarinyl peptide substrates were purchased from Enzo Life Sciences.

Protein Expression and Purification. To generate the HDAC8 construct used for crystallization, the codon-optimized HDAC8 gene was amplified from the previously described HDAC8-His₆-pET20b construct¹ (primers: forward – 5'-TACTTCCAATCCAATGCAGACTCTGGGCAGTCTCTG-3'; reverse – 5'-TTATCCACTTCCAATGTTATTACCTCATTTCAGGTTGCC). This was cloned into the pET His6 MBP TEV LIC cloning vector (1M), a gift from Scott Gradia (University of California, Berkeley; Addgene plasmid #29656), in-frame with a TEV-cleavable N-terminal His-MBP-tag (MBP; maltose binding protein) using ligation independent cloning.

The HDAC8 construct bearing a C-terminal hexahistidine tag (HDAC8_{His}) was used for all experiments except where otherwise noted. Wild-type and mutant HDAC8_{His} expression was performed as previously described¹ with minor modifications. Briefly, 50 mL starting cultures were grown overnight in Lysogeny Broth (LB) in the presence of 100 $\mu\text{g}/\text{mL}$ ampicillin. These were inoculated into 12 \times 1 L M9 minimal media with 100 $\mu\text{g}/\text{ml}$ ampicillin at 37°C. When the OD₆₀₀ reached ~ 1.0 , expression was induced at 18°C for wild-type and 16°C for mutants by adding 200 μM ZnCl₂ (Hampton Research) and 100 μM isopropyl- β -thiogalactopyranoside. After

expression for 18–21 h, cells were pelleted via centrifugation and stored at -80°C until purification. HDAC8_{His} was purified as previously described.¹ All protein was concentrated over 10 kDa molecular weight cut-off centrifugal filters (Millipore) to 8–20 mg/mL. Protein concentrations were determined from the absorbance at 280 nm using the molar extinction coefficient $50,240\text{ M}^{-1}\text{cm}^{-1}$. Aliquots were flash-cooled in liquid nitrogen and stored at -80°C .

The His-MBP-TEV-HDAC8 construct, consisting of Ser-Asn followed by residues 8-374 of human HDAC8 and thus designated "HDAC8₃₇₄", was used for crystallography. HDAC8₃₇₄ was expressed in the same manner as HDAC8_{His}, the only difference being that 50 $\mu\text{g}/\text{mL}$ kanamycin was used in place of 100 $\mu\text{g}/\text{mL}$ ampicillin. This construct was purified using a modified version of the protocol described for similar constructs of HDAC6.² Briefly, cells were resuspended and lysed by sonication in loading buffer [50 mM Tris (pH 8.0), 300 mM KCl, 5% glycerol, 1 mM TCEP] and applied to amylose resin (New England Biolabs). Protein was eluted with 10 mM maltose and incubated with recombinant His-tobacco etch virus protease (TEVP) at 4°C overnight. The cleaved protein was run over Ni(II)-NTA resin (Qiagen). His-MBP and His-TEVP were eluted with 400 mM imidazole and removal of these proteins was verified using SDS-PAGE. If separation was less than satisfactory, flow-through fractions were subjected to a second Ni(II)-NTA column. HDAC8₃₇₄-containing fractions were then concentrated via centrifugation to 5-10 mL and loaded onto a HiLoad SuperDex 200 column (GE Healthcare) in size exclusion buffer [50 mM Tris (pH 8.0), 150 mM KCl, 5% glycerol, 1 mM TCEP]. Purified HDAC8₃₇₄ was concentrated to 10-20 mg/mL and flash-cooled in liquid nitrogen for storage at -80°C .

The HDAC8₃₇₄ construct appeared to exhibit somewhat lower activity than HDAC8_{His} with specific activities of 1030 ± 10 and 1530 ± 30 (nmol P) \cdot ($\mu\text{mol E}$)⁻¹ \cdot min⁻¹, respectively. However, ITC measurements of trapoxin A binding to both HDAC8 constructs reveal identical dissociation constants ($K_d = 3 \pm 1$ nM) but lower N values for the same concentration of

enzyme, suggesting that HDAC8₃₇₄ may be slightly Zn²⁺ deficient following purification (Supporting Information Figure S6).

C153S HDAC8_{His} Mutagenesis. The C153S mutation was introduced in the HDAC8-His₆-pET20b construct¹ using Quikchange site-directed mutagenesis (Agilent Technologies). The forward primer sequence used was 5'-GCTTCTGGTTTCTCTTACCTGAACGATGCC-3' and the reverse primer sequence was 5'-GGCATCGTTCAGGTAAGAGAAACCAGAAGC-3'. The PCR product was sequenced at the Genomics Analysis Core to confirm the mutation. This mutant was expressed and purified using the same protocol outlined for HDAC8_{His} presented above. Plasmids for H142A and Y306F HDAC8_{His} were utilized from previously reported studies.³

Crystallization. The HDAC8₃₇₄-trapoxin A complex was cocrystallized in a sitting drop using the vapor diffusion method at 4°C. HDAC8₃₇₄ (5 mg/mL) was incubated with 400 µM trapoxin A in size exclusion buffer with 1% DMSO at room temperature for 1 h. A 350 nL drop was then combined with 350 nL of precipitant solution (35% dioxane) and equilibrated against an 80 µL reservoir of precipitant solution. Large triangular prism crystals were observed after 3 d. Crystals were immersed in a cryoprotectant solution comprised of mother liquor supplemented with 15% ethylene glycol before being flash-cooled in liquid nitrogen.

Crystal Structure Determination. X-ray diffraction data were collected at the Stanford Synchrotron Radiation Lightsource (SSRL), beamline 9-2. Data reduction and integration were carried out using iMosflm⁴ and scaled using Aimless in the CCP4 suite of programs;⁵ crystallographic and refinement statistics are recorded in Supporting Information Table S1. Molecular replacement was executed using the atomic coordinates of H143A HDAC8 (PDB ID: 3EWF)¹ without ligands as a search model in Phaser.⁶ Coot was used to build and adjust the model in the electron density map, and refinement was performed with Phenix.^{7,8} Trapoxin A, dioxane, ethylene glycol, and water molecules were added in later stages of refinement. Occasional spurious electron density peaks were present that could not be unambiguously

modeled by solvent or other additives present during crystallization, so these were left uninterpreted. The quality of the final model was evaluated with MolProbity and PROCHECK.^{9,10} Multiple conformations were observed for E23, S43, V82, C102, T105, D147, E148, S150, L155, S190, M196, S204, S215, L235, K239, Q242, S246, C275, M279, S328, D333, T349, S351, and C352. Electron density was ambiguous or absent for the D87-I94 segment in the L2 loop as well as part or all of the side chains of L14, V15, K58, K60, E106, so these were omitted from the final model.

Inhibitor Reversibility Dialysis Assay. To assess the reversibility of cyclic tetrapeptide inhibition, 300 μL samples were prepared of 10 μM HDAC8_{His} with no inhibitor, 100 μM trapoxin A, or 100 μM apicidin in size exclusion buffer supplemented with 0.25% DMSO. These were incubated at room temperature for 1 h and then transferred into 10 kDa MWCO Slide-a-Lyzer cassettes (Thermo Scientific) and dialyzed against 3 L of size exclusion buffer at 4°C. After 6 h, 100 μL was extracted from each cassette and the remaining 200 μL was dialyzed against 2 L of fresh size exclusion buffer overnight.

After the initial 1 h incubation, as well as the first and second round of dialysis, a standard discontinuous coupled fluorogenic assay was run to assess enzyme activity using the *Fluor de Lys* HDAC8 tetrapeptide assay substrate Ac-Arg-His-Lys(Ac)-Lys(Ac)-aminomethylcoumarin (BML-KI178-0005; Enzo Life Sciences). Lysine deacetylation by HDAC8 was measured by cleavage of the amide bond with the aminomethylcoumarin group by trypsin, resulting in red-shifted fluorescence. This signal was then fit to a standard curve to quantify product concentration.

Assays were performed in triplicate at room temperature. HDAC8_{His} was diluted to 1 μM in size exclusion buffer and the assay substrate was diluted to 300 μM in activity assay buffer [25 mM Tris (pH 8.2), 137 mM NaCl, 2.7 mM KCl, and 1 mM MgCl₂]. Then, 25 μL of enzyme and 25 μL of substrate were mixed and incubated at room temperature in the dark for 30 min. The reaction was quenched by the addition of 50 μL assay buffer containing trypsin and 200 μM

suberoylanilide hydroxamic acid (SAHA; Cayman Chemical), a pan-HDAC inhibitor. Following 30 min of development in the dark, fluorescence was measured using a Tecan Infinite M1000Pro plate reader ($\lambda_{\text{ex}} = 360 \text{ nm}$, $\lambda_{\text{em}} = 460 \text{ nm}$). Specific activity assays of wild-type HDAC8_{His} and HDAC8₃₇₄ were performed in the same manner and processed using a standard curve generated by correlating known product concentrations with the signal following trypsin digestion. Data were averaged and plotted using GraphPad Prism.

Isothermal Titration Calorimetry. Experiments were performed with wild-type and Y306F HDAC8_{His}, as well as wild-type HDAC8₃₇₄, for both trapoxin A and apicidin while H142A and C153S HDAC8_{His} were studied with trapoxin A only (Supporting Information Figure S6). Heat curves were measured using a MicroCal iTC200 isothermal titration calorimeter (Malvern). For trapoxin A, 200 μM inhibitor was titrated against 20 μM enzyme in size exclusion buffer containing 0.5% DMSO. Due to the limited solubility of apicidin in aqueous media, 100 μM inhibitor was titrated against 10 μM enzyme in size exclusion buffer with 5% DMSO. Forty 1- μL injections were made over 80 min except for the titration of apicidin against Y306F HDAC8_{His}. This experiment used twenty 2- μL injections over 1 h to increase the observed heat per injection. Integration, curve fitting, and figure generation were performed using Origin (OriginLab, Northampton, MA).

Matrix-Assisted Lased Desorption/Ionization (MALDI) Mass Spectrometry. MALDI mass spectrometry was used to verify the modification state of a sample of 50 μM HDAC8_{His} incubated with 500 μM trapoxin A at 37°C for 18 h prior to its submission for LC-MS/MS analysis. After incubation, 2 μL were removed and mixed with 10 μL of saturated sinapic acid (Sigma-Aldrich) in 50:50 acetonitrile:0.1% aqueous trifluoroacetic acid and then a 2 μL sample of the resulting solution was transferred to a 384-spot steel MALDI target plate (Bruker). Once the matrix had crystallized and the spots were dry, mass spectra were obtained on a Bruker Ultraflex III TOF/TOF mass spectrometer with 2000 shots per spot at 50% laser power. Data

were processed in flexAnalysis (Bruker Daltonics) and mass spectra were plotted in GraphPad Prism (Supporting Information Figure S3).

Tryptic Peptide Liquid Chromatography-Tandem Mass Spectrometry (LC-MS/MS).

LC-MS/MS was used to search for sites of modification of HDAC8 by trapoxin A, focusing on His and Cys residues since the closest potential nucleophiles to the epoxide in the HDAC8 complex were H142 and C153. Runs of LC-MS/MS were carried out on HDAC8_{His} alone in size exclusion buffer as a control as well as samples consisting of (1) 480 μ M HDAC8_{His} with 480 μ M trapoxin A, (2) 50 μ M HDAC8_{His} with 200 μ M TpxA, and (3) 50 μ M HDAC8_{His} with 500 μ M TpxA. Samples 1 and 2 were incubated at room temperature for 1 h while sample 3 was incubated at 37°C for 18 h. Peaks consistent with mono- and di-labeled HDAC8_{His} with TpxA were observed for sample 3 by MALDI prior to LC-MS/MS analysis (Supporting Information Figure S3).

LC-MS/MS was carried out at the Wistar Institute Proteomics and Metabolomics Facility. Samples were reduced with 15 mM TCEP for 30 min and then alkylated with 15 mM iodoacetamide for 45 min. The reaction was quenched by incubation with 35 mM L-cysteine for 15 min prior to tryptic digestion. The samples were digested with trypsin overnight in the absence of denaturant. LC-MS/MS data were collected on a Q Exactive HF mass spectrometer. MaxQuant 1.5.2.8 was used to search mass spectra against the UniProt *E. coli* database plus the sequence of HDAC8_{His} allowing for N-terminal acetylation, Met oxidation, Asn deamidation, C carbamidomethylation, and a mass addition of 602.3 Da at His or Cys residues corresponding to modification by trapoxin A. Modification by trapoxin A was observed at 6 sites in run 1, 10 sites in run 2, and 15 sites in run 3 (4 of which were His residues in the hexahistidine tag).

Liquid Chromatography-Mass Spectrometry (LC-MS). LC-MS was used to determine the observed mass of HDAC8 in the presence and absence of trapoxin A. Previously, it had been proposed that trapoxin A covalently modifies the enzyme in the folded state, but upon denaturation it is hydrolyzed from the enzyme.¹¹ A sample of 200 μ M trapoxin A was incubated in size exclusion buffer plus 0.5% DMSO for 1 h with and without 200 μ M HDAC8₃₇₄. A 50 μ L

aliquot of each sample was then diluted with 50 μL of acetonitrile, filtered via centrifugation, and submitted to LC-MS analysis. A 2 μL aliquot was then injected over a C_{18} reverse phase column with a gradient from 95:5 water:acetonitrile to 5:95 water:acetonitrile on a Waters Acquity UPLC-MS. Mass spectra were processed using MassLynx software (Waters) and plotted using GraphPad Prism.

Table S1. Data collection and refinement statistics for the HDAC8₃₇₄–trapoxin A complex

HDAC8 ₃₇₄ –trapoxin A	
<i>Unit Cell</i>	
Space group	<i>P</i> 3 ₂
<i>a</i> , <i>b</i> , <i>c</i> (Å)	50.98, 50.98, 116.52
α , β , γ (°)	90.0, 90.0, 120.0
<i>Data Collection</i>	
Wavelength (Å)	0.97949
Resolution (Å)	44.15–1.24
Total/unique no. of reflections	456789/95873
R _{merge} ^{a,b}	0.046 (0.592)
R _{p.i.m.} ^{a,c}	0.035 (0.440)
CC _{1/2} ^{a,d}	0.999 (0.671)
I/σ(I) ^a	13.7 (2.2)
Redundancy ^a	4.8 (4.7)
Completeness (%) ^a	99.1 (99.7)
<i>Refinement</i>	
No. of reflections used in refinement/test set	95808 / 9680
R _{work} ^{a,e}	0.121 (0.209)
R _{free} ^{a,e}	0.143 (0.253)
No. of nonhydrogen atoms:	
protein	2912
ligand	108
solvent	383
Average <i>B</i> -factors (Å ²)	
protein	17
ligand	22
solvent	30
Root-mean-square deviation from ideal geometry	
bonds (Å)	0.009
angles (°)	1.0
Ramachandran plot (%) ^f	
favored	98.1
allowed	1.9
PDB accession code	5VI6

^aValues in parentheses refer to data in the highest shell. ^bR_{merge} = $\sum_{hkl} \sum_i |I_{i,hkl} - \langle I \rangle_{hkl}| / \sum_{hkl} \sum_i I_{i,hkl}$, where $\langle I \rangle_{hkl}$ is the average intensity calculated for reflection *hkl* from replicate measurements. ^cR_{p.i.m.} = $(\sum_{hkl} (1/(N-1))^{1/2} \sum_i |I_{i,hkl} - \langle I \rangle_{hkl}|) / \sum_{hkl} \sum_i I_{i,hkl}$, where $\langle I \rangle_{hkl}$ is the average intensity calculated for reflection *hkl* from replicate measurements and *N* is the number of reflections. ^dPearson correlation coefficient between random half-datasets. ^eR_{work} = $\sum ||F_o| - |F_c|| / \sum |F_o|$ for reflections contained in the working set. |F_o| and |F_c| are the observed and calculated structure factor amplitudes, respectively. R_{free} is calculated using the same expression for reflections contained in the test set held aside during refinement. ^fCalculated with PROCHECK.¹⁰

Table S2. Trapoxin A-modified Cys and His residues detected by LC-MS/MS in each run. N_{obs} refers to the total number of times that a residue was observed. N_{mod} refers to the number of times that the residue was detected with a mass addition consistent with trapoxin A modification.

	Run 1		Run 2		Run 3	
[HDAC8 _{His}] (uM)	480		50		50	
[trapoxin A] (uM)	480		200		500	
Incubation	RT* for 1 hour		RT* for 1 hour		37°C for 18 hours	
Residue	N_{obs}	N_{mod}	N_{obs}	N_{mod}	N_{obs}	N_{mod}
H42	—————		207	5	170	6
H51	21	2	207	2	170	11
H71	—————		223	2	228	1
H78	77	1	—————		228	1
C102	11	2	—————		—————	
H142	—————		157	14	—————	
H143	—————		157	1	63	2
C153	27	2	—————		—————	
H180	—————		—————		112	2
H201	22	1	—————		42	5
C244	51	1	100	2	46	1
C275	—————		89	2	11	1
C314	—————		98	1	—————	
H334	—————		98	2	—————	
C352	—————		98	4	43	10
H375	—————		12	1	14	4
HisTag	—————		—————		20	10

*RT = room temperature.

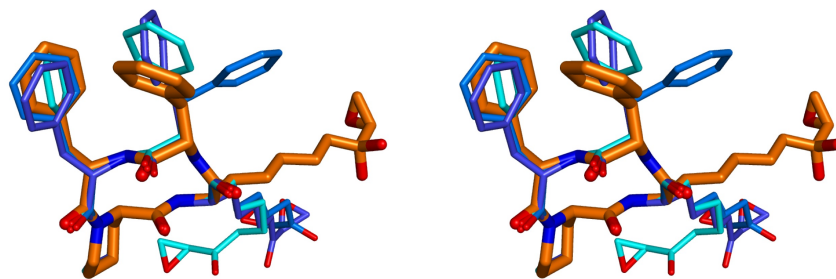


Figure S1. Stereoview of the conformation of trapoxin A as bound to HDAC8 (orange) superimposed on the three molecules in the asymmetric unit of the uncomplexed trapoxin A crystal structure (CSD ID: TALDEP; cyan, light blue, blue). The side chain conformation of L-Aoe in the uncomplexed inhibitor differs from that observed in the enzyme-bound inhibitor.

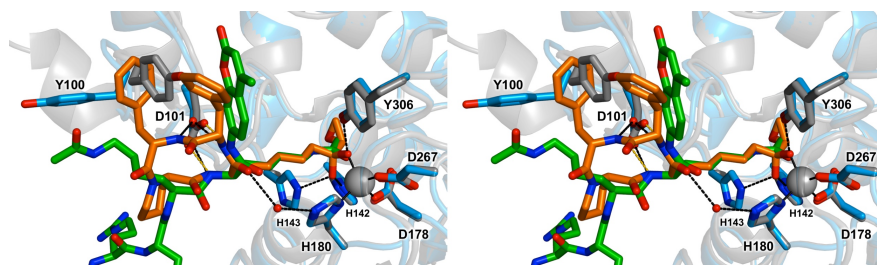


Figure S2. Stereoview of the superposition of trapoxin A (orange) bound to HDAC8 (blue ribbon) and the coumarinyl peptide substrate RHK(Ac)K(Ac)-aminomethylcoumarin (green) bound to H143A HDAC8 (grey ribbon; PDB ID: 3EWF).¹ Selected residues are labeled. Metal coordination interactions are shown as black lines, hydrogen-bonds with trapoxin A are shown as black dashes, and the D101-substrate hydrogen bonds are shown as gold dashed lines. A water-mediated hydrogen bond is observed between the L-Aoe carbonyl of trapoxin A and the imidazole side chain of H180, a metal-binding residue. Trapoxin A binding causes parts of the L2 loop to become disordered and Y100 to rotate outward. One major conformation of Y100 is observed, but residual electron density suggests the presence of another minor conformation making a favorable edge-to-face interaction with a Phe side chain of trapoxin A.

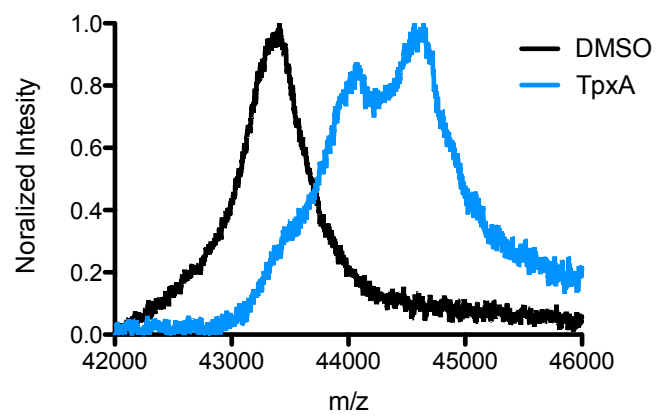


Figure S3. MALDI mass spectra of HDAC8_{His} incubated with DMSO (black) or trapoxin A (TpxA, blue) at 37°C for 18 h prior to LC-MS/MS experiment.

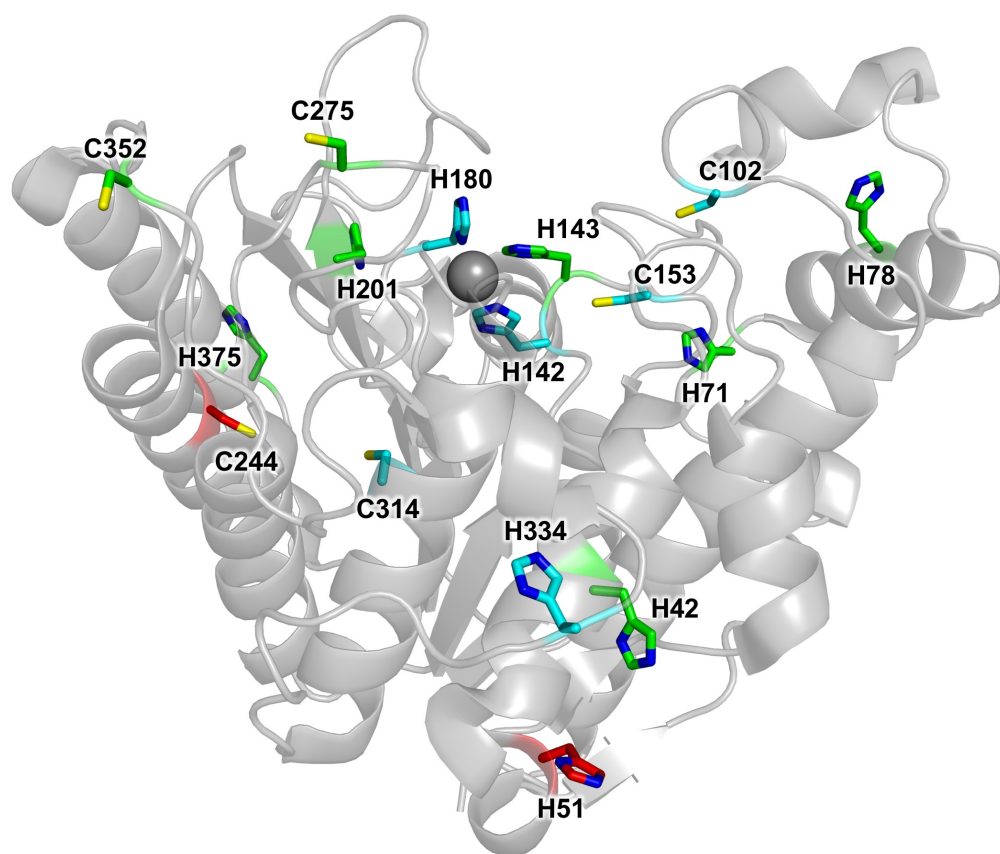


Figure S4. Sites at which covalent modification by trapoxin A was detected by LC-MS/MS. Of the 17 sites modified, 16 are shown here because one site of modification, the hexahistidine tag, is disordered and hence not observed in the crystal structure. Color coding indicates sites observed in one (cyan), two (green), or three (red) replicates. Modification percentages are shown in Supporting Information Table S2. Only H51 and C244 were modified in all trials, with total modification fractions ranging from 1.5–9.5%. The only sites with modification fractions exceeding 20% in a single trial were surface residues C352, H375, and residues in the hexahistidine tag at levels of 23%, 29%, and 50%, respectively. Only sporadic labeling of tandem catalytic histidine residues H142 and H143, zinc ligand H180, and C153 was observed in one or two trials, with modification fractions ranging 0.6–9.0% for any one of these residues.

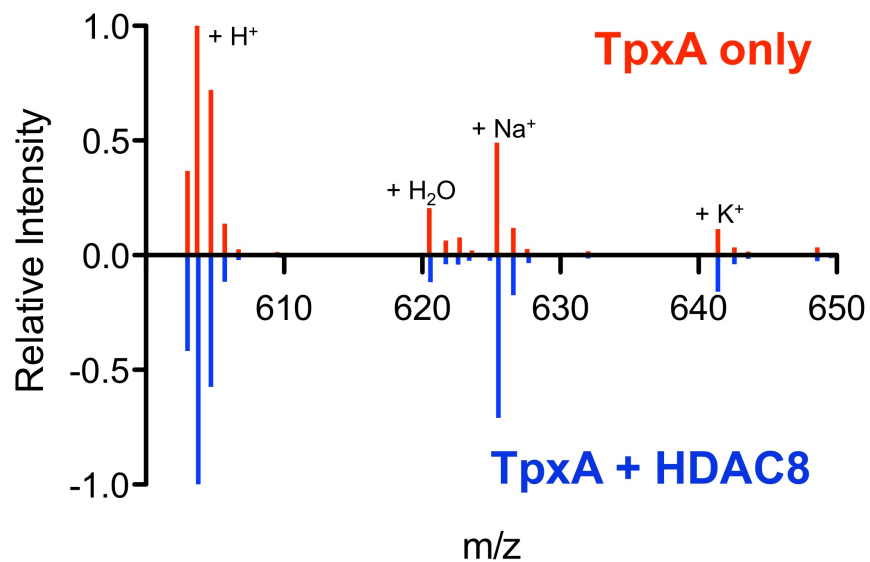


Figure S5. Normalized mass spectra of trapoxin A (TpxA) incubated in the presence (blue) and absence (red) of HDAC8. Monoisotopic mass peaks corresponding to the mass of trapoxin A plus a proton, sodium ion, water, and potassium ions are labeled. Interestingly, an additional peak is observed in mass spectra of both samples that is consistent with monohydrated trapoxin A. This could reflect the enhanced reactivity of the α,β -epoxyketone carbonyl resulting in a higher percentage of the gem-diol in solution.

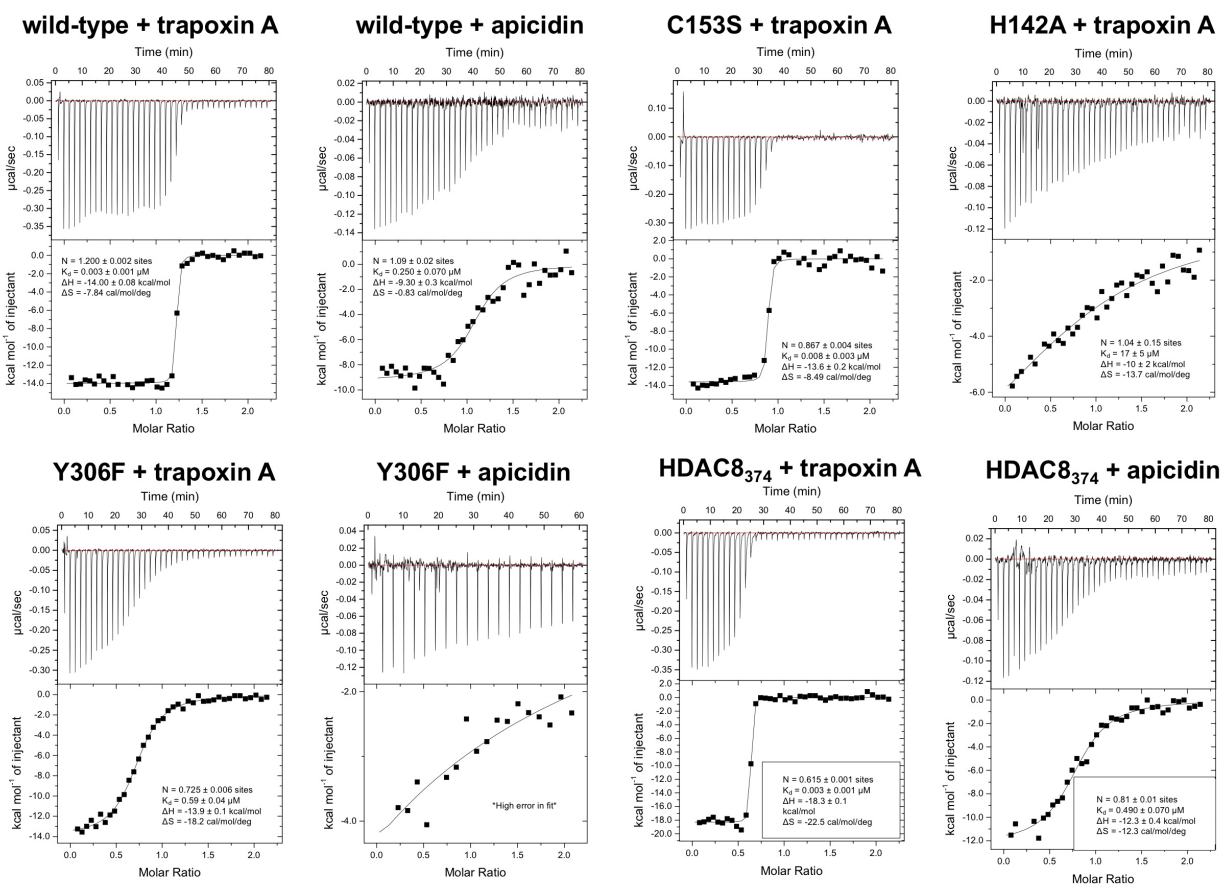


Figure S6. ITC thermograms and corresponding binding isotherms derived from integrating thermograms using the one-site model. Measurements were made for: 200 µM trapoxin A versus 20 µM wild-type, H142A, C153S, and Y306F HDAC8; and 100 µM apicidin versus 10 µM wild-type and Y306F HDAC8. The HDAC8 construct bearing the hexahistidine tag, HDAC8_{His}, was used for these measurements. The wild-type tagless construct, HDAC8₃₇₄, was also studied with trapoxin A and apicidin using identical conditions. Thermodynamic constants for each run are calculated from curve fitting and inlaid in each plot.

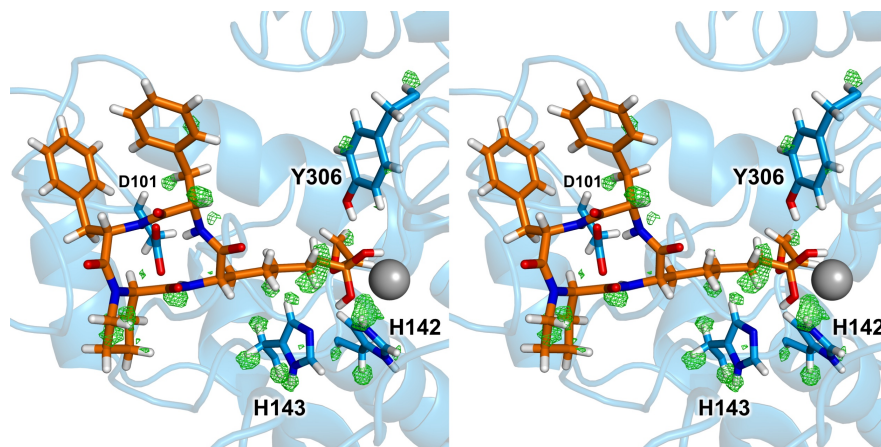


Figure S7. Stereoview of a simulated annealing omit map contoured at 2.5σ showing hydrogen atoms in the HDAC8-trapoxin A complex. The zinc ion is indicated by a gray sphere. A large electron density peak corresponds to the N_{ϵ} -H atom of H142, indicating that this residue is in the positively charged imidazolium state.

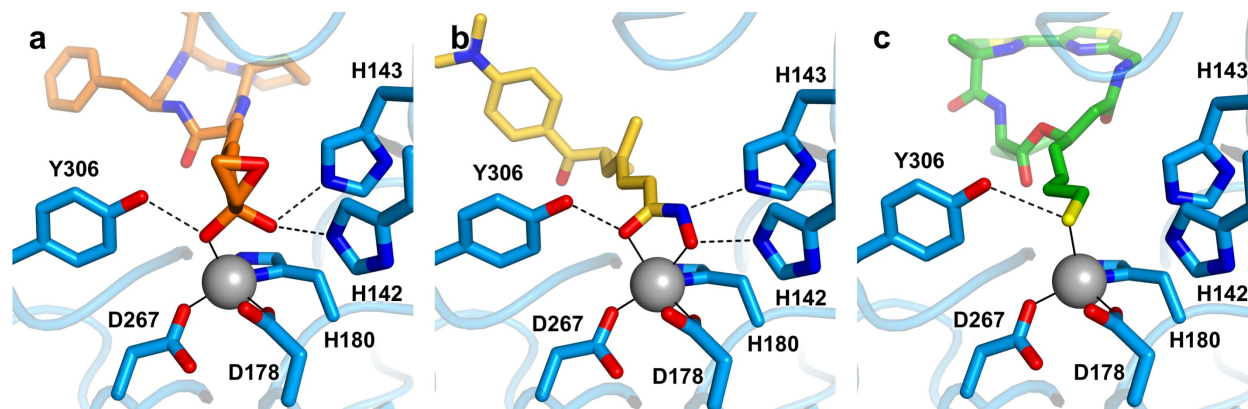


Figure S8. Zinc coordination interactions in HDAC8–inhibitor complexes. (a) HDAC8–trapoxin A complex (current work), PDB 5VI6. (b) HDAC8–trichostatin A complex, PDB 1T64. HDAC8–largazole complex, PDB 3RQD.

References

1. Dowling, D. P., Gantt, S. L., Gattis, S. G., Fierke, C. A., and Christianson, D. W. (2008) Structural studies of human histone deacetylase 8 and its site-specific variants complexed with substrate and inhibitors. *Biochemistry* 47, 13554–13563.
2. Hai, Y. and Christianson, D.W. (2016) Histone deacetylase 6 structure and molecular basis of catalysis and inhibition. *Nat. Chem. Biol.* 12, 741–747.
3. Gantt, S. L., Decroos, C., Lee, M. S., Gullet, L. E., Bowman, C. M., Christianson, D. W., and Fierke, C. A. (2016) General base-general acid catalysis in human histone deacetylase 8. *Biochemistry* 55, 820–832.
4. Battye, T. G. G., Kontogiannis, L., Johnson, O., Powell, H. R., and Leslie, A. G. W. (2011) iMosflm: a new graphical interface for diffraction-image processing with Mosflm. *Acta Cryst. D67*, 271–281.
5. Winn, M. D., Ballard, C. C., Cowtan, K. D., Dodson, E. J., Emsley, P., Evans, P. R., Keegan, R. M., Krissinel, E. B., Leslie, A. G. W., McCoy, A., McNicholas, S. J., Murshudov, G. N., Pannu, N. S., Potterton, E. A., Powell, H. R., Read, R. J., Vagin, A., and Wilson, K. S. (2011) Overview of the CCP4 suite and current developments. *Acta Cryst. D67*, 235–242.
6. McCoy, A. J., Grosse-Kunstleve, R. W., Adams, P. D., Winn, M. D., Storoni, L. C., and Read, R. J. (2007) *Phaser* crystallographic software *J. Appl. Cryst.* 40, 658–674.
7. Emsley, P., Lohkamp, B., Scott, W. G., and Cowtan, K. (2010) Features and development of Coot. *Acta Cryst. D66*, 486–501.
8. Adams, P. D., Afonine, P. V., Bunkóczi, G., Chen, V. B., Davis, I. W., Echols, N., Headd, J. J., Hung, L., Kapral, G. J., Grosse-Kunstleve, R. W., McCoy, A. J., Moriarty, N. W., Oeffner, R., Read, R. J., Richardson, D. C., Richardson, J. S., Terwillinger, T. C., and Zwart, P. H. (2010) PHENIX: a comprehensive Python-based system for macromolecular structure solution. *Acta*

Cryst. D66, 213–221.

9. Chen, V. B., Arendal III, W. B., Headd, J. J., Keedy, D. A., Immormino, R. M., Kapral, G. J., Murray, L. W., Richardson, J. S., and Richardson, D. C. (2010) MolProbity: All-atom structure validation for macromolecular crystallography. *Acta Cryst. D66*, 12–21.
10. Laskowski, R. A., MacArthur, M. W., Moss, D. S., and Thornton, J. M. (1993) PROCHECK: A program to check the stereochemical quality of protein structures. *J. Appl. Cryst.* 26, 283–291.
11. Taunton, J., Collins, J. L., and Schreiber, S. L. (1996) Synthesis of natural and modified trapoxins, useful reagents for exploring histone deacetylase function. *J. Am. Chem. Soc.* 118, 10412–10422.